Temperature dependence of formation and shrinkage of hollow shells in hemispherical Ag/Pd nanoparticles

Journal:	*Philosophical Magazine & Philosophical Magazine Letters*
Manuscript ID:	TPHM-12-Jan-0007.R1
Journal Selection:	Philosophical Magazine
Date Submitted by the Author:	n/a
Complete List of Authors:	Glodan, Gyorgyi; University of Debrecen, Department of Solid State Physics Cserhati, Csaba; University of Debrecen, Department of Solid State Physics Beke, Dezso; University of Debrecen, Department of Solid State Physics
Keywords:	diffusion, TEM, nanostructured materials
Keywords (user supplied):	hollow nanostructures, stability, Kirkendall effect

Temperature dependence of formation and shrinkage of hollow shells in hemispherical Ag/Pd nanoparticles

György Glodán[a], Csaba Cserháti[a] and Dezső L. Beke[a *]

[a]Department of Solid State Physics, University of Debrecen, 4010 Debrecen, P.O.Box. 2, Hungary

*Corresponding author. E-mail: dbeke@delfin.unideb.hu

Temperature dependence of formation and shrinkage of hollow shells in hemispherical Ag/Pd nanoparticles

György Glodán[1)], Csaba Cserháti [1)] and Dezső L. Beke [1)]
[1)]*Department of Solid State Physics, University of Debrecen, 4010 Debrecen, P.O.Box. 2, Hungary*

It is shown that both the growth and shrinkage of hollow shells in Ag/Pd hemispherical core-shell nano structures took place at the same temperature. The crossover time, t_{cr}, between these regimes is shifted to smaller values with increasing temperatures. This result confirms that the growth and the shrinkage regimes are controlled by the faster as well as the slower diffusion coefficients (D_{Ag} as well as D_{Pd}), respectively. The pore radius, confirming recent theoretical predictions, linearly depends on the initial particle radius and the slope of this straight line increases with the average composition of the faster component.

Keywords: hollow nanostructures; stability; interdiffusion; Kirkendall effect

1. Introduction

The synthesis of hollow nanostructures (nanospheres, nanotubes) have promising properties for new types of possible applications such as recoverable catalysts, drug delivers, photonic devices, nano-chemical reactors etc. [1-13]. In most of the cases the formation of nanospheres or nanotubes was based on the solid state diffusion and/or reaction between two parent materials and the Kirkendall effect was applied to explain the formation of holes in the core, containing the fast diffusing element.

Indeed it was shown theoretically that the formation stage of pores inside a core/shell (A/B) nanosphere was controlled by the diffusion coefficient of the fast diffusion component [3,4,9,12]; a resultant vacancy flow, J_v, oriented to the A core, arises because $J_A>J_B$ ($D_A>D_B$, D_i are the diffusion coefficients). Although the details of the nucleation and growth of the void(s) can be complicated due to different additional effects (stress development [4,10,14], non-steady state vacancy distribution [12], etc.) it is generally accepted that the overall growth of the hole is controlled by D_A and $t_g \sim R_o^2/D_A$ was obtained for the time to complete the shell formation [4, 11] (R_o is the initial particle radius).

On the other hand the above nanoshell structure should be unstable due to the Gibbs-Thomson effect [6,7], creating an outward vacancy flux leading to shrinkage. In binary systems the so called inverse Kirkendall effect should also influence the shrinkage [7,8]. Indeed it was obtained in [7] that the shrinking time (during which the radius of the hole decreases to the R_{ho}/e value, where e is the base of the natural logarithm and R_{ho} is the initial hole radius) can be given as

$$t_{shr} \sim (kT/\gamma\Omega)\,(R_f^3/D_A)[(1-c_A)D_A/D_B+c_A]. \quad (1)$$

R_f is the final particle radius after collapse, k and T have their usual meaning, c_A is the atomic fraction of A, γ and Ω denote the surface energy and the atomic volume, respectively. If $D_A/D_B>>1$, $t_{shr} \sim R_f^3/D_B$. In recent theoretical papers [8,9,11,12,15,16] it is shown that, in

binary systems with wide mutual solubility range and for relatively not too large $D_A/D_B(\cong 10)$ ratios, first there is a relatively fast growing stage which is followed by a slower shrinkage process at the same temperature. This behaviour was experimentally illustrated in Ag/Au system [10], where an Ag-50%Au solid solution has been formed in the shell and the shrinkage took place at the same temperature. All earlier experimental investigations were carried out in systems, where the shell was a reaction product and the shrinkage process was observed *at higher temperatures* than at which they were formed (see e.g. [13] where Ni and Cu oxide nanoshells were produced by oxidation of pure metallic particles).

In a very recent theoretical paper [11] the growth and shrinkage process in one run was investigated in both spherical and cylindrical geometry. It was found that the maximal pore radius, corresponding to the crossover time, t_{cr}, between the two regimes, depended (almost linearly) on the initial particles radius, R_o, and on the average concentration. Unfortunately the effect of the annealing temperature was not simulated.

In this communication we report experimental results on the temperature dependence of the porosity formation and shrinkage in Ag/Pd hemisphere sells.

2. Experimental

Separated hemisphere beads of Ag were produced as described in [10]. The average initial radius, of the Ag islands was about 20 nm as well as 10 nm for two different sets of samples. Thin Pd film (of about 10-20nm) was evaporated on the top of ensembles of Ag beads. The initial average radii of the Ag/Pd hemispherical particles, R_o, was about 40 as well as 27 nm (Set 1 and Set 2, respectively) with a dispersion of about 35% (Fig. 1).

The specimens were annealed at 703K, 723K and 743K for 10, 20, 30, 60, 120 and 180 minutes in dynamic reducing gas flow (5%H+95%Ar mixture). After heat treatments the beads were removed from the sapphire substrate by tearing off the dried film formed by dropping collodion (solution of nitrocellulose in alcohol) solution onto the surface. The dried film was placed with the top side onto a TEM grid covered with amorphous carbon layer. After the dissolution of the carrier (collodion) layer the bottom side of the beads was investigated by JEOL 2000FX-II TEM/EDX system at 200keV on plan view.

The area of the holes and beads were measured by standard image processing method: the edges of the beads and pores were detected at several points. The points were then connected with straight lines and the area of this polygon had been measured in nm^2.

Fig. 2 shows examples of the hollow islands obtained at 743K, 723K and 703K after 20 minutes. The formed pores have circular or polygonal shape. Usually less than tree pores (but mostly only one pore) were evolved during the heat treatments. Note, that an opposite phenomena was observed in the Ag-Au system; many small pores were observed at the lowest annealing temperature, similarly as predicted by computer simulations [7] and observed also during Co sulphide shell formation [4].

Fig. 3 shows the ratio of the area of the pore (a) and particle (A) versus the annealing time at different temperatures for Set 1. This kind of presentation is beneficial, because the area ratio clearly mimics the volume or radius ratio and because the initial size of our beads showed a size distribution ($a/A \sim R_p/R_e$, where and R_p and R_o are the pore radius and the external radius of the shell). The functions in Fig. 3 are similar to the same plots obtained the in Ag/Au system [1] and it is in accordance with predictions of theoretical papers [9,11,12]: the envelope curves have the maximum at the crossover time, t_{cr}, between the growth and shrinkage regimes. However, in contrast to [10], where we could not draw a definite conclusion on the temperature dependence of t_{cr}, the temperature dependence of t_{cr} can be

clearly seen in Fig. 3: the position of the maximum is shifted to longer times with decreasing temperature. At 743K the maximum should be at about 10 minutes, i.e. the formation of pores was too fast to be observed (see the dashed line in Fig. 3).

In both of our experiments (in this one and also in [10]) a distribution of beads was present. Thus it was possible to plot the pore radius, R_p, as the function of the external radius, R_e, belonging to the maxima of the relative pore area versus time functions. Linear relations were obtained in [10] for *a* versus *A* (or R_p versus R_e) functions with similar slopes for both temperatures investigated. In Fig. 4, in order to make easier the comparison with recent theoretical predictions [11], the radius of the pore at t_{cr}, versus the actual (external) radius of the particles, are plotted directly in this system. In spite of the high experimental scatter of the points, the functions at a fixed annealing temperature can be fitted with a linear function. Increasing the temperature the slope of the linear function also increases. (In Fig. 4, for the shake of clarity, the points belonging to the intermediate temperature, 723K, are not shown, but they lie between the two straight lines).

Having two sample sets, with different initial average radii, R_o, we can also investigate whether the slopes of the R_p versus R_e functions are the same in these two ensembles or not. Fig. 5 shows these two functions at 743K. The points can be fitted by straight lines, with different slopes: the difference in slopes is about a factor of two.

3. Discussion and conclusions

It can be seen in Fig. 3 that the time corresponding to the maxima of the curves, t_{cr}, shifts to smaller values with increasing temperature. According to theoretical estimations for larger t_g/t_{shr} ratio the crossover time should be shorter, i.e. $t_{cr} \sim t_{shr}/t_g \sim (R^3_f/R_o^2) D_A/D_B \cong R_o D_A/D_B$ (due to conservation of matter $(R_f/R_o)^3 \cong 1$, i.e. $R_f \cong R_o$.) Since $D_A >> D_B$ and, as a general rule, the diffusion activation energy for the slower component is larger than the faster one ($Q_B > Q_A$);

$$t_{cr} \sim \exp[(Q_B - Q_A)/kT\ ], \qquad (2)$$

if R_o is constant. This indeed gives decreasing t_{cr} values with increasing temperatures. Thus we can conclude that the temperature dependence of the crossover time observed is in accordance with the theoretical result that the growth and the shrinkage processes are controlled by the faster as well as slower diffusing components, respectively.

It follows from the previous arguments that if D_A and D_B differs considerably, (e.g. $D_A >> D_B$ i.e. $D_A/D_B > 10^3$) then the shrinkage process can be observed only at higher temperatures than the temperature at which their formation was observed. This seems to be the case for oxide nanoshells or nanotubes formed by oxidation of metallic particles [13,17]. If the D_A/D_B ratio is not considerably larger than unity then, being the times t_{shr} and t_g close values, the two stages can be observed in one run, but the wide maximum on the R_p versus t plots does not have a well recognizable shift with the temperature. This was the case in the Ag/Au system (see Fig. 2. in [10]). For intermediate values of D_A/D_B the two stages can be still observable at the same temperature and the temperature dependence of the crossover time can also be observed. Let us see numerical values for the diffusion coefficients. According to data collection [18] $D_{AginAg}/D_{AuinAg} \cong 9$ while $D_{AginAg}/D_{PdinAg} \cong 300$ at 740 K. Obviously these ratios are composition dependent and e.g. $D_{AginAu}/D_{AuinAu} \cong 2$ (there are no experimental for D_{AginPd}), but their average value of this ratio over the whole composition range is still should differ by about a factor of 5. Thus one can conclude that indeed in the Ag/Au system the two stages should be not far from each other, while in the Ag/Pd system the growth and shrinkage

times are different enough to allow the observation of the temperature dependence of the crossover time.

Theoretical calculations in [11] resulted in a linear dependence of the pore radius, R_p, at the crossover moment, as the function of the initial particle radius (R_o). From our experimental data we were able to calculate the above pore radius as the function of the actual (external) particle radius, R_e. However, according to the conservation of volume, $R_e^3=R_o^3+R_p^3$, and following a similar approximation used also in [7], i.e. $R_o-R_p=\Delta R<R_o$, one can write:

$$R_e^3 \cong 2R_o^3\{1-(3/2(\Delta R/R_o)[1-\Delta R/R_o]\}, \text{ i.e. } R_e \sim R_o. \quad (3)$$

Thus our results, shown in Fig. 4, can be interpreted as the experimental confirmation of the linear relation between R_p and R_o (see also Fig. 3 in [11]). Moreover, we can also conclude from our results that the slope of this straight line has definite temperature dependence: the slope increases with increasing temperature.

The results shown in Fig. 5 are also interesting. At first sight it seems to be surprising why the slopes of the straight lines, fitted to the two ensembles with different average initial radii, differ. The smaller slope can be interpreted as follows. In [11] it was shown that the slope of the R_p versus R_o functions depends on the average composition of the faster component, c_A, as well. It was obtained (Fig. 4 in [11]) that the slope was smaller for lower average value of c_A. In our experiments the average composition of the formed AgPd solid solutions could be different for the two groups with different average initial radii. Indeed, according to the Energy Dispersive X-ray analysis (EDX) in TEM, the Ag content was about 65at% as well as 54at% in the hollow hemispherical shells in the sets with larger and smaller average radius, respectively. Thus the silver content should be less for particles with smaller initial radius and thus, in accordance with the calculations [11], the slope for this group should be smaller too.

Acknowledgments

This work was supported by Grant No. CK 80126 of the Hungarian Scientific Research Found and and by the TAMOP 4.2.1./B-09/1/KONV-2010-007 project, which is co-financed by the European Union and European Social Fund.

References

[1] Y. Sun, B. Mayers, Y. Xia, Nano Lett. 2 (2002) p. 481
[2] Y. Sun, B. Mayers, Y. Xia, Adv. Mater. 25 (2003) p. 641
[3] Y.Yin, R.M. Rioux, C.K. Erdonmez, S. Hughes, G,A, Somorjai, A.P. Alivisatos, Science 304 (2004) p. 711
[4] Y. Yin, C.K. Erdonmez, A. Cabot, S. Hughes, A.P. Alivisatos, Adv. Func. Mater. 16 (2006) p. 1389
[5] H.J. Fan, M. Knez, R. Scholtz, D. Hesse, K. Nirelsch. M. Zacharias, U. Gössele, Nano Lett. 7 (2007) p. 993
[6] K. N. Tu, U. Gössele, Appl. Phys. Lett. **86** (2005) p. 093111
[7] A.M. Gusak. T.V Zaporozhets, K.N. Tu, U. Gössele, Phil. Mag. 85 (2005) p. 4445
[8] A.V. Evteev, A.V. Levchenko, I.V. Belova, G.E. Murch, Phil. Mag. 88 (2008) p. 1525
[9] A.M. Gusak, T.V. Zaporozhets, J. Phys. Condens. Matter. 21 (2009) p. 415303
[10] Gy. Glodán, Cs. Cserhati, I. Beszeda, D.L. Beke, Appl. Phys. Lett. 97 (2010) p. 113109
[11] O.M. Podolyan, T.V. Zaporozhets, Ukr. J. Phys. 56 (2011) p. 929

[12] G.E. Murch, A.V. Evteev. E.V. Levtheko, I,V, Belova, Diffus. Fundam. 42 (2009) p. 1
[13] R. Nakamura, D. Tokozakura, J.-G.Lee, H. Mori, H. Nakajima, Acta Mater. 56 (2008) p. 5276
[14] J. Svoboda, F.D. Fisher, Acta Mater. 59 (2011) p. 61
[15] A.M. Gusak, K.N. Tu, Acta Mater. 57 (2009) p. 3367
[16] A.V. Evteev, A.V. Levchenko, I.V. Belova, G.E. Murch, J. of Nano Res. 7 (2009) p. 11
[17] R. Nakamura, G. Matsubayashi, H. Tsuchiya, S. Fujimoto, H. Nakajima, Acta Mater. 57 (2009) p. 5046
[18] H. Mehrer (editor): Diffusion in Solid Metals and Alloys, Landolt Börnstein, New Series III/26, Springer-Verlag, Berlin, 1990

Figure captions:
Fig. 1 Size distribution of the initial Ag/Pd hemispherical particles for the two sets of samples.

FIG 2: TEM picture of Ag-Pd hemispheres formed at a) 743 K, b) 723 K and c) 703 K for 20 minutes annealing time

FIG 3: Relative area of the pores as the function of the annealing time at 703K (square), 723K (triangle) and 743K (circle) for Set 1. The experimental points were obtained by averaging over 10-30 particles.

FIG 4: Hole radius, R_p, at the crossover time as the function of the actual (external) radius, R_e, of the beads for 703 K (square) and 743 K (circle) (a, b, c are the slopes of the linear functions at 743, 723 and 703K, respectively) for Set 1.

FIG 5: Hole radius, R_p, at the crossover time as the function of the actual (external) radius, R_e, at 743K for the two sets of samples with different initial sizes (a, and b are the slopes of the linear functions, belonging to the bigger (circle) and smaller (triangle) average initial sizes, respectively).

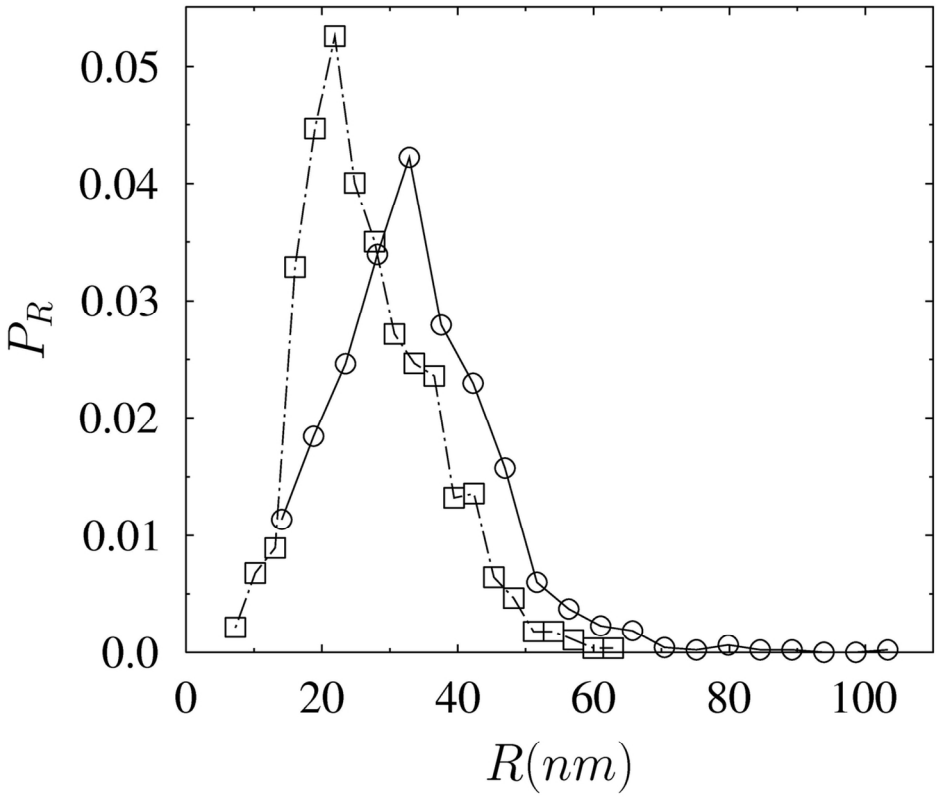

Size distribution of the initial Ag/Pd hemispherical particles for the two sets of samples.
120x103mm (300 x 300 DPI)

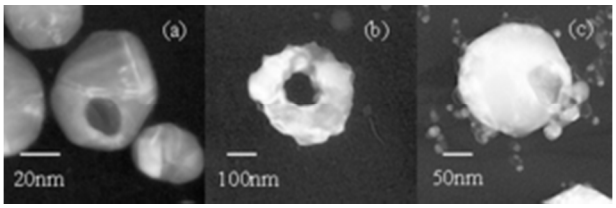

25x8mm (300 x 300 DPI)

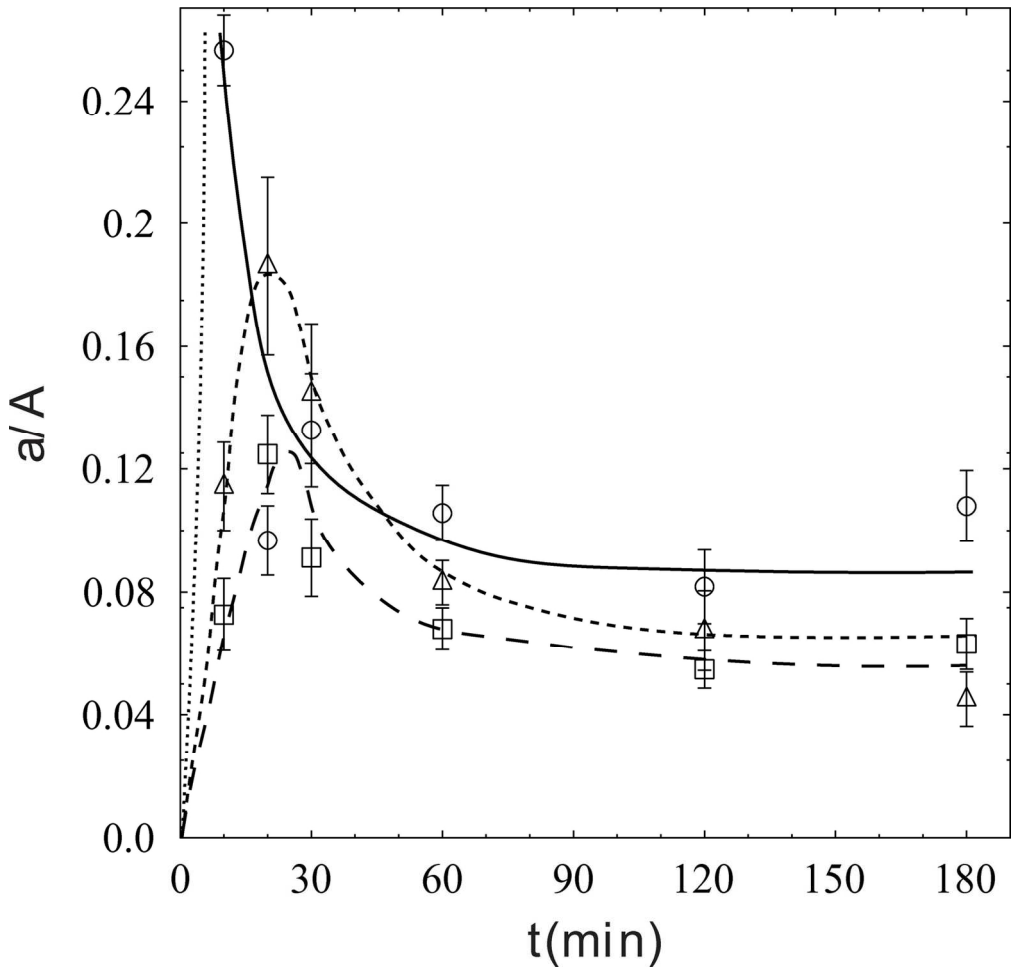

Relative area of the pores as the function of the annealing time at 703K (square), 723K (triangle) and 743K (circle) for Set 1. The experimental points were obtained by averaging over 10-30 particles.
145x139mm (300 x 300 DPI)

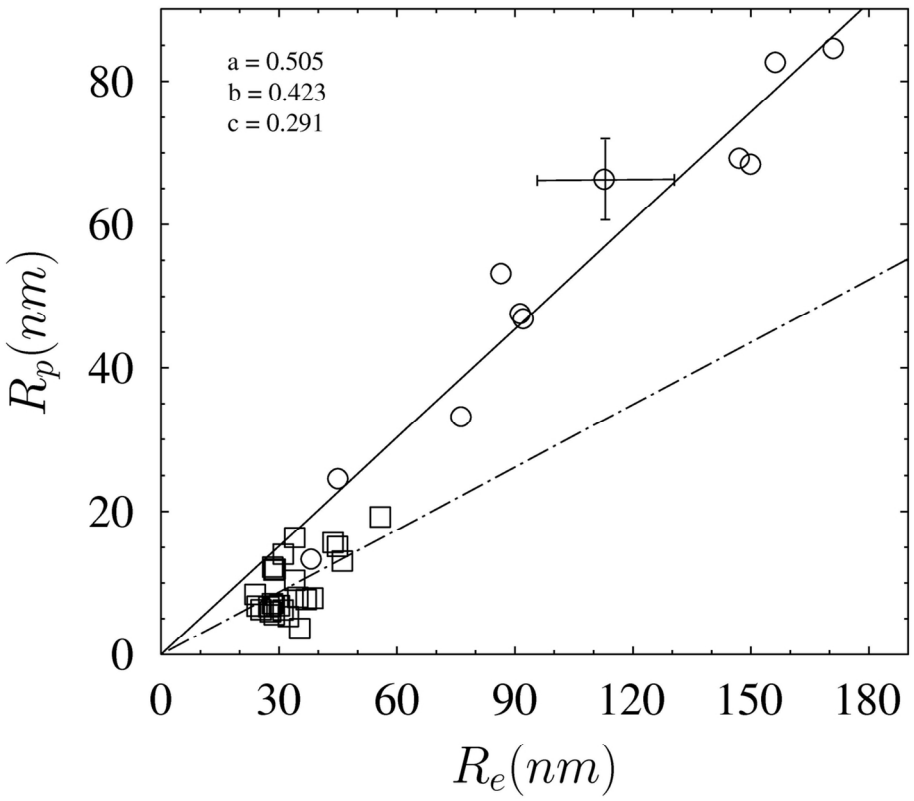

Hole radius, Rp, at the crossover time as the function of the actual (external) radius, Re, of the beads for 703 K (square) and 743 K (circle) (a, b, c are the slopes of the linear functions at 743, 723 and 703K, respectively) for Set 1.
120x103mm (300 x 300 DPI)

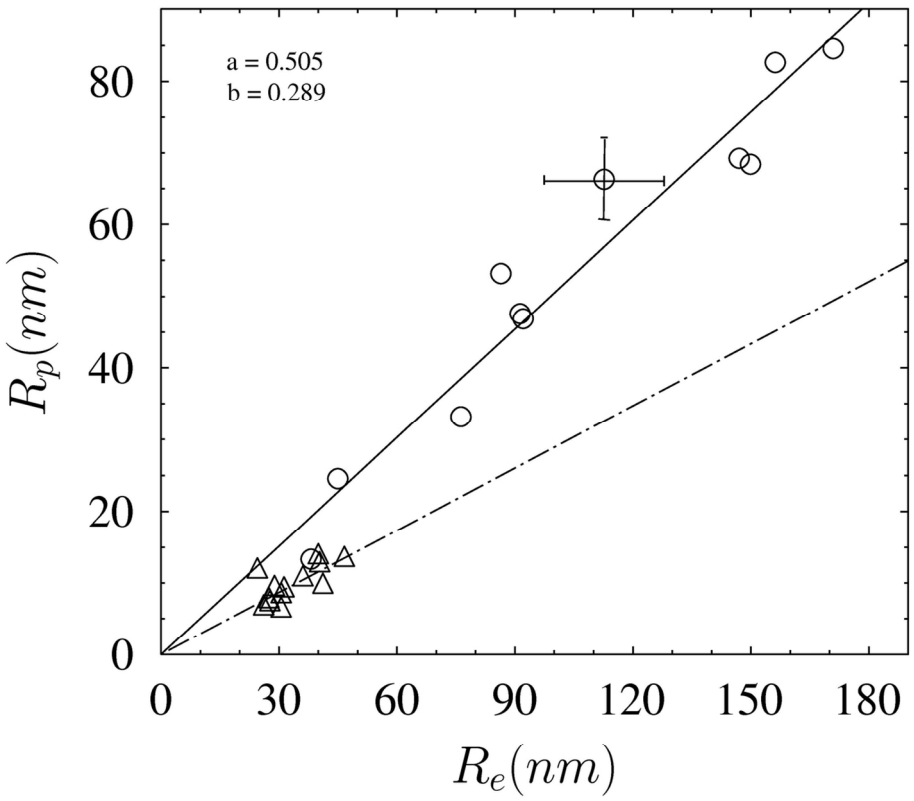

Hole radius, Rp, at the crossover time as the function of the actual (external) radius, Re, at 743K for the two sets of samples with different initial sizes (a, and b are the slopes of the linear functions, belonging to the bigger (circle) and smaller (triangle) average initial sizes, respectively).
120x103mm (300 x 300 DPI)